



北京大学物理学院
School of Physics, Peking University

CGSM and MBPT calculations with realistic nuclear forces

Furong Xu

Outline

I. Core Gamow Shell Model (CGSM) with CD Bonn

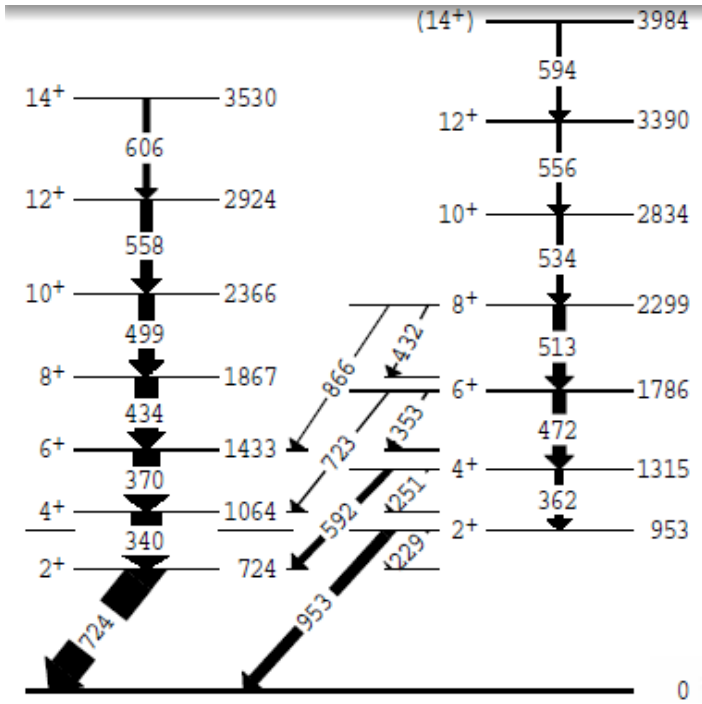
(resonance + continuum)

II. *Ab-initio* MBPT with $N^3\text{LO}$ (LQCD)

NTSE-2016, Khabarovsk, 19-23 September, 2016, Khabarovsk, Russian

γ -ray spectra

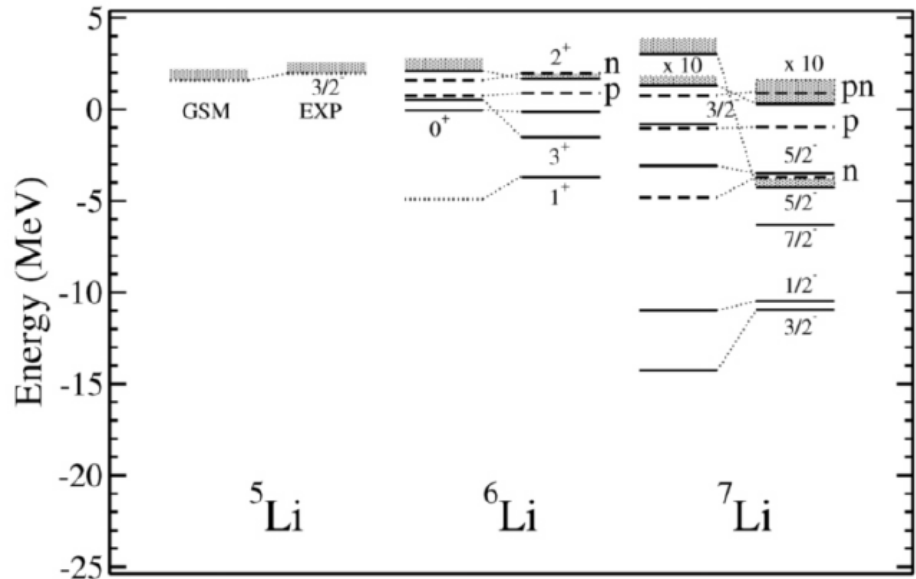
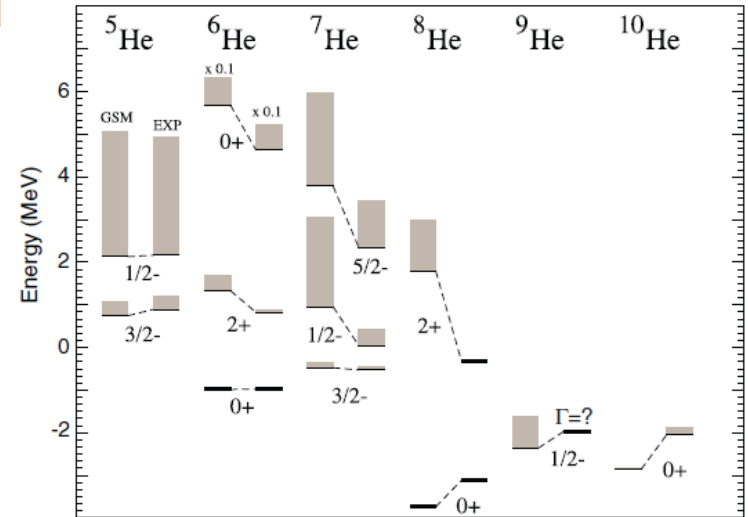
^{188}Pb : prolate and oblate bands



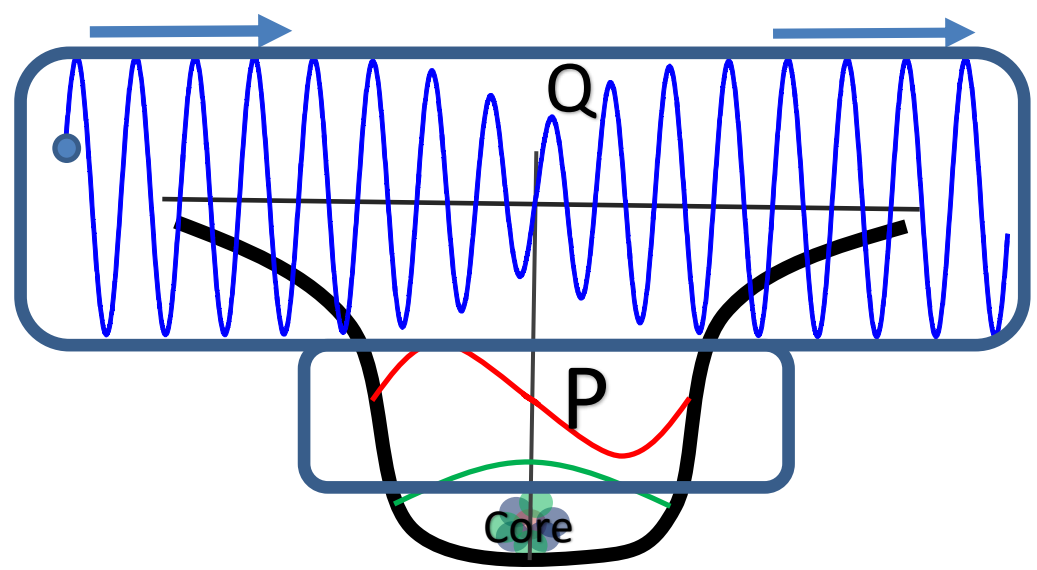
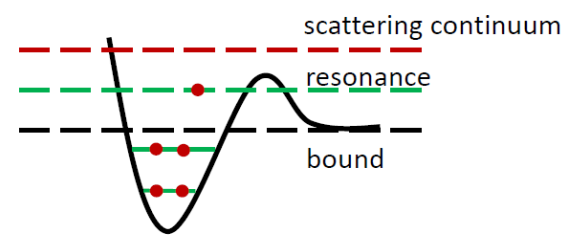
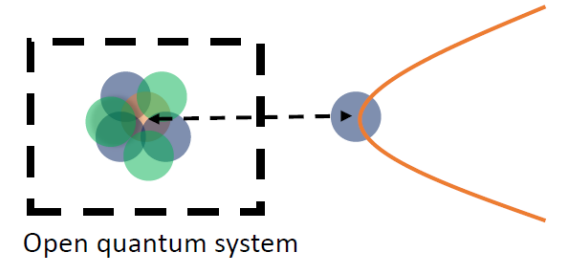
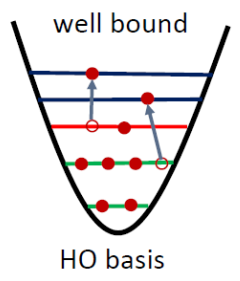
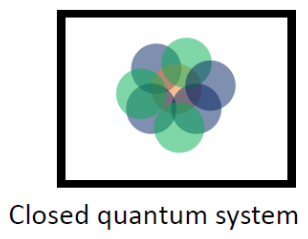
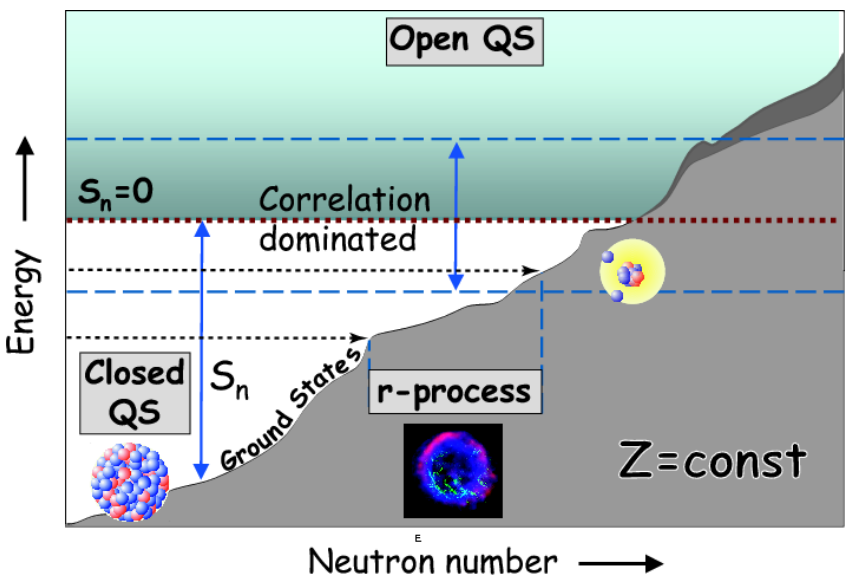
J. Pakarinen et al., PRC 72,
011304(R) (2005)

Spectra of resonance states

Energies and lifetimes or widths (against particle emissions)



N. Michel, W. Nazarewicz, J. Okolowicz, M. Ploszyczak, Nucl. Phys. A 752, 335c (2005)



Gamow Shell Model

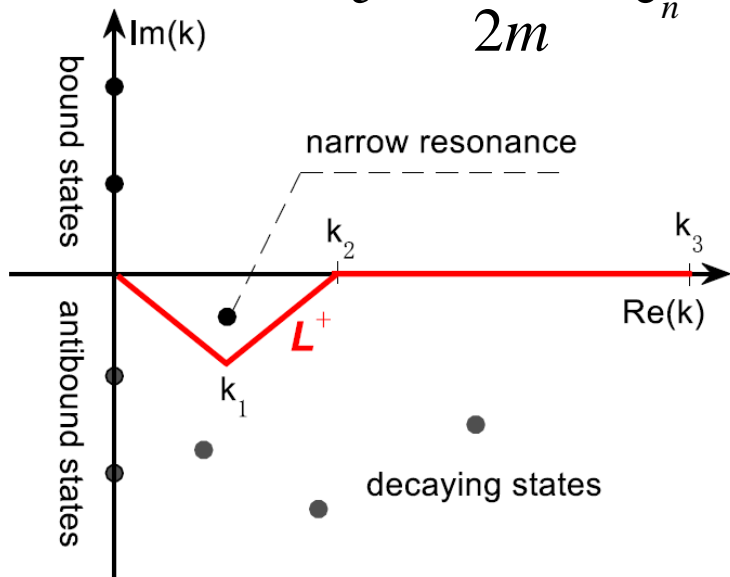
T. Berggren, Nucl. Phys. A109 (1968) 265

Single-particle Berggren basis in complex- k plane, describing bound, resonance and scattering on equal footing.

The radial wave function $u(r)/r$

$$\frac{d^2 u(k, r)}{dr^2} = \left(\frac{\ell(\ell + 1)}{r^2} + \frac{2m}{\hbar^2} V(r) - k^2 \right) u(k, r)$$

$$e = \frac{\hbar^2 k^2}{2m} = e_n - i \frac{\gamma_n}{2}$$



boundary conditions

$$u(0) = 0,$$

$$u(a)O_i'(ka) - u'(a)O_i(ka) = 0$$

$$O_i(kr) \sim e^{i(kr - l\pi/2)}$$

Outgoing solution at large distance

Orthogonality and Completeness

$$\delta(r - r') = \sum_n w_n(r, k_n) w_n(r', k_n)$$

$$+ \frac{1}{\pi} \int_{L^+} dq u(r, q) u(r', q)$$

Discretized

R.J. Liotta *et al.*, PLB 367, 1 (1996)...

Used Berggren basis to describe single-particle resonance in nuclei;

later for **two-particle** resonance (Betan *et al.*, PRL 89, 042601 (2002))

Using phenomenological potential

For many-body systems

$$H = \sum_{i=1}^A \frac{p_i^2}{2m} + \sum_{i<j=1}^A v_{ij}^{NN} - \frac{P^2}{2Am}$$

$$H = \sum_{i=1}^A \frac{p_i^2}{2m} + U + \sum_{i<j=1}^A \left(v_{ij}^{NN} - U - \frac{p_i^2}{2Am} - \frac{\mathbf{p}_i \mathbf{p}_j}{Am} \right)$$

$$= H_0 + V.$$

U is the Woods-Saxon potential

$$E = E_n - i \frac{\Gamma_n}{2}$$

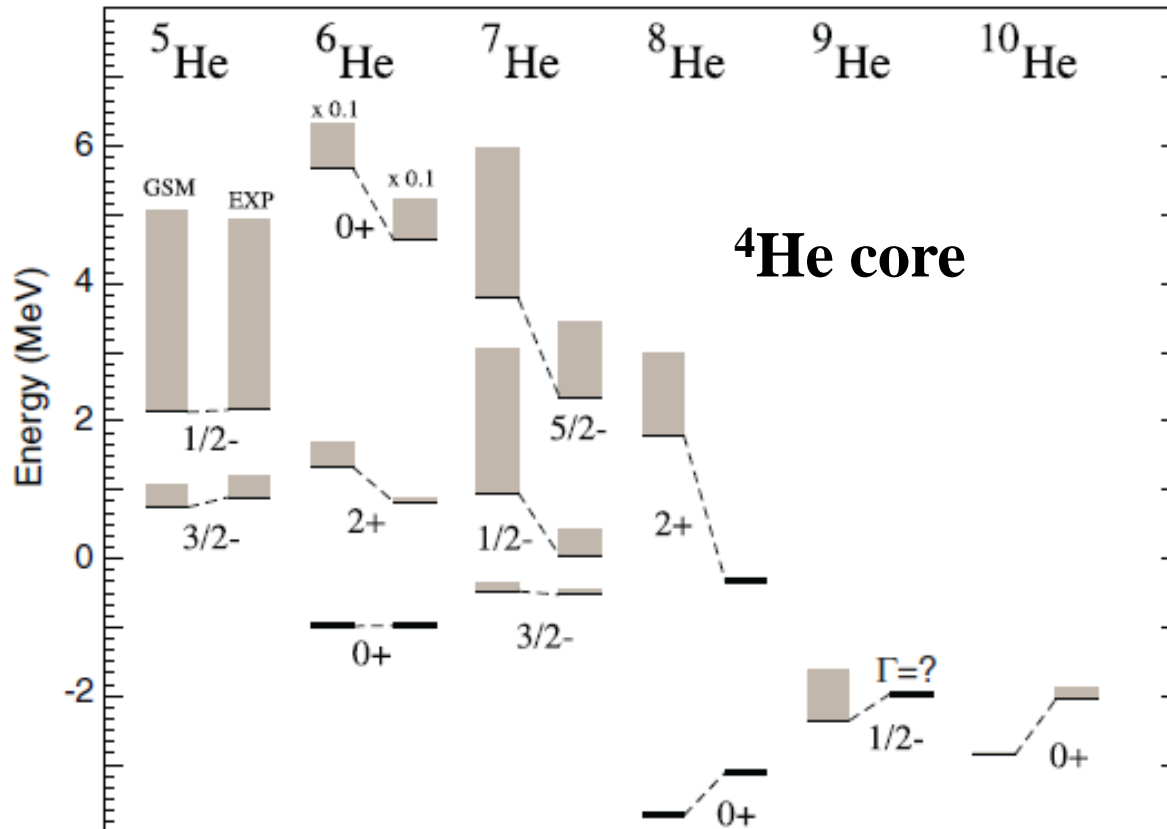
Michel, Nazarewicz, Płoszajczak, Rotureau *et al.*, 2003--

$$V = V_{WS} + V_{J,T}(\vec{r}_1, \vec{r}_2)$$

phenomenological potential

$$V(\mathbf{r}_i, \mathbf{r}_j) = -V_{SGI}^{(J,T)} \exp \left[- \left(\frac{r_i - r_j}{\mu} \right)^2 \right] \delta(r_i + r_j - 2R_0)$$

$V_{SGI}^{(J)}$ is the strength in the JT channel



Michel, Nazarewicz,
Płoszajczak, Vertse,
Phys. G: Nucl. Part. Phys.
36 (2009) 013101

Hagen, Hjorth-Jensen *et al.*, PRC 73, 064307 (2006): Core GSM

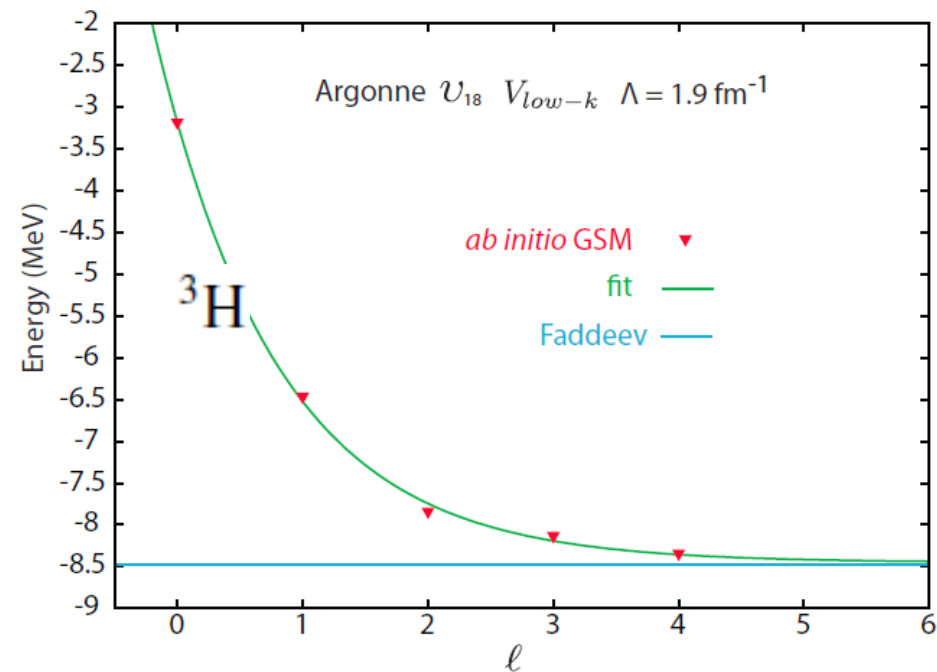
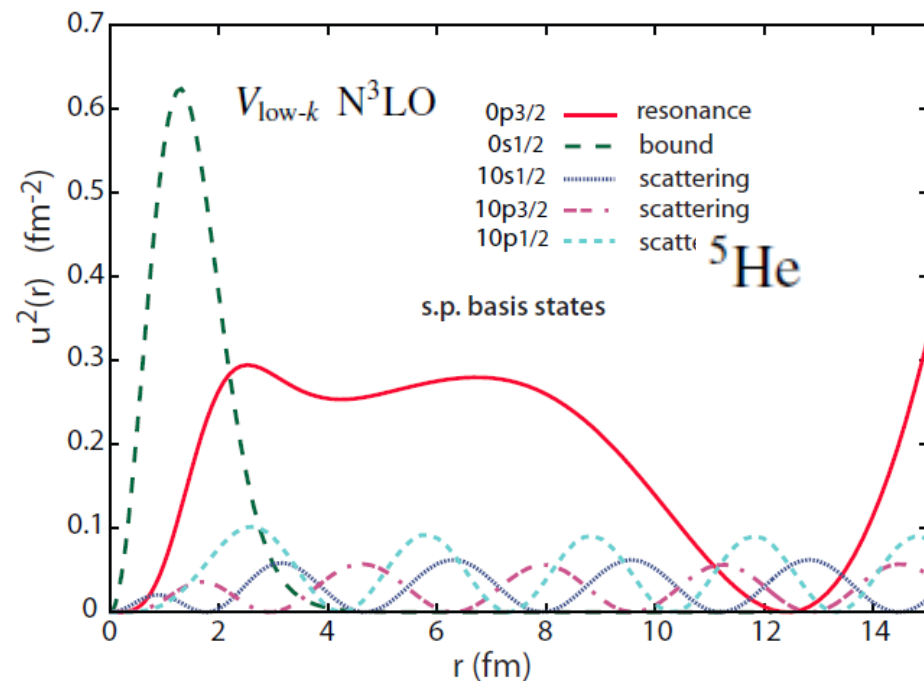
with realistic nuclear forces, but no Q-box, limited to 2 valence particles;

later Tsukiyama Hjorth-Jensen, Hagen, PRC 80, 051301 (R) (2009) improved

by using Q-box but not folded diagrams, limited to 2 or 3 valence particles

Papadimitriou *et al.*, Phys. Rev. C 88, 044318 (2013): realistic nuclear forces

Ab initio no-core Gamow shell model calculations for light nuclei



Our Gamow shell model with an inert core

- 1. To start from realistic nuclear forces;**
- 2. No limitation on the number of valence particles;**

Q-box + folded diagrams

- 3. To calculate level energies + resonance widths of states.**

Realistic CGSM with CD-Bonn

Realistic nuclear forces \rightarrow Gamow shell model calculations

Taking a doubly closed core

Bare forces:
Strong repulsion,
slow convergence

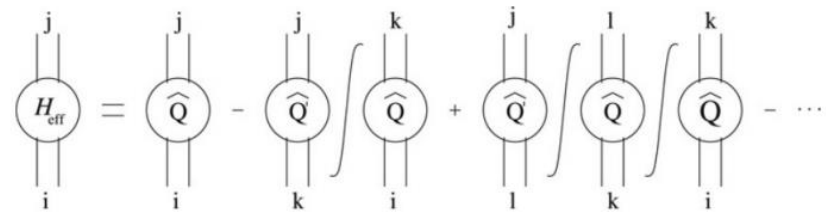
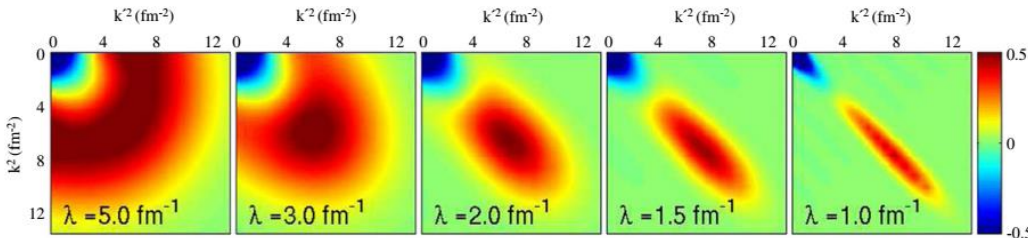
$V_{low k}$ or SRG

To remove hard core,
but still keep good
descriptions of NN
scattering phase shifts

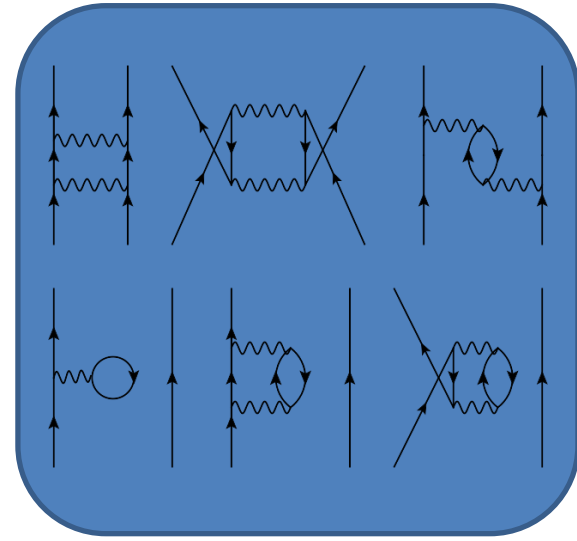
$$\langle \alpha_P | \bar{H}_{\text{eff}} | \alpha_{P'} \rangle = \sum_{\alpha_{P''}} \sum_{\alpha_{P'''}} \sum_{kk'} \sum_{k''k'''} \langle \alpha_P | \tilde{k}'' \rangle \langle \tilde{k}'' | \alpha_{P''} \rangle \langle \alpha_{P''} | \tilde{k} \rangle E_k \langle \tilde{k} | \alpha_{P'''} \rangle \langle \alpha_{P'''} | \tilde{k}' \rangle \langle \tilde{k}' | \alpha_{P'} \rangle$$

$$\frac{dH_\lambda}{d\lambda} = -\frac{4}{\lambda^5} [[T_{\text{rel}}, H_\lambda], H_\lambda]$$

Q



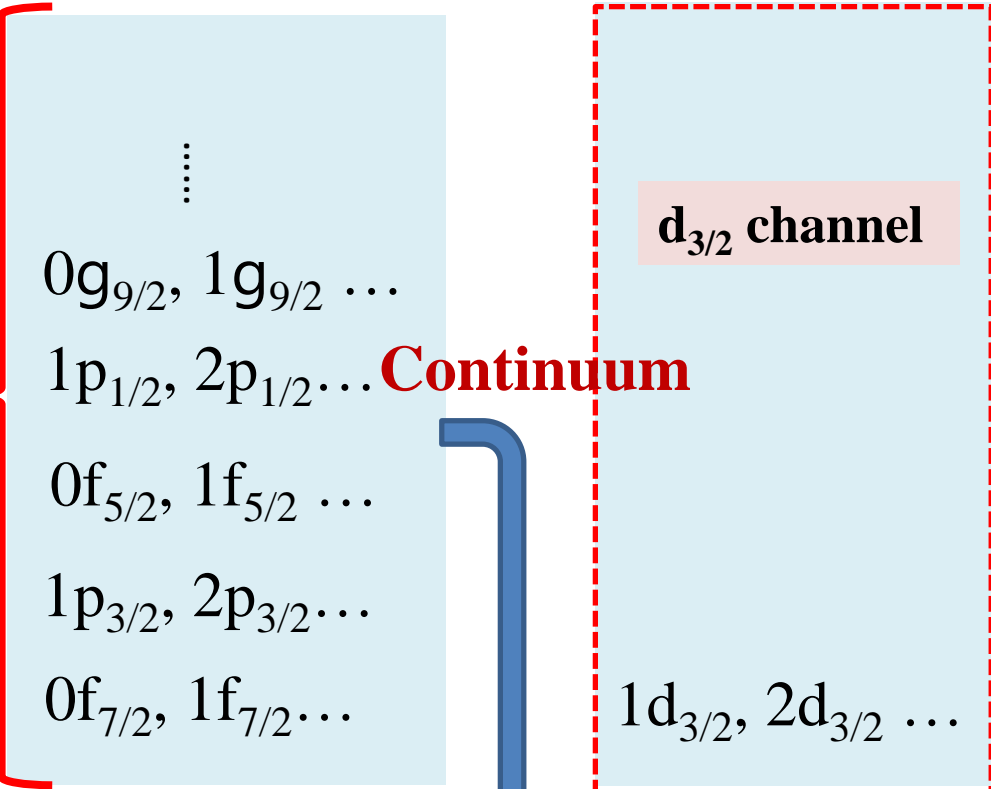
$$\hat{Q}(E) = PVP + PVQ \frac{1}{E - H} QVP;$$



Nondegenerated extended Kuo-Krenciglowa folded-diagram method (EKK) by Takayanagi, NPA 852, 61 (2011)

Model space

Continuum



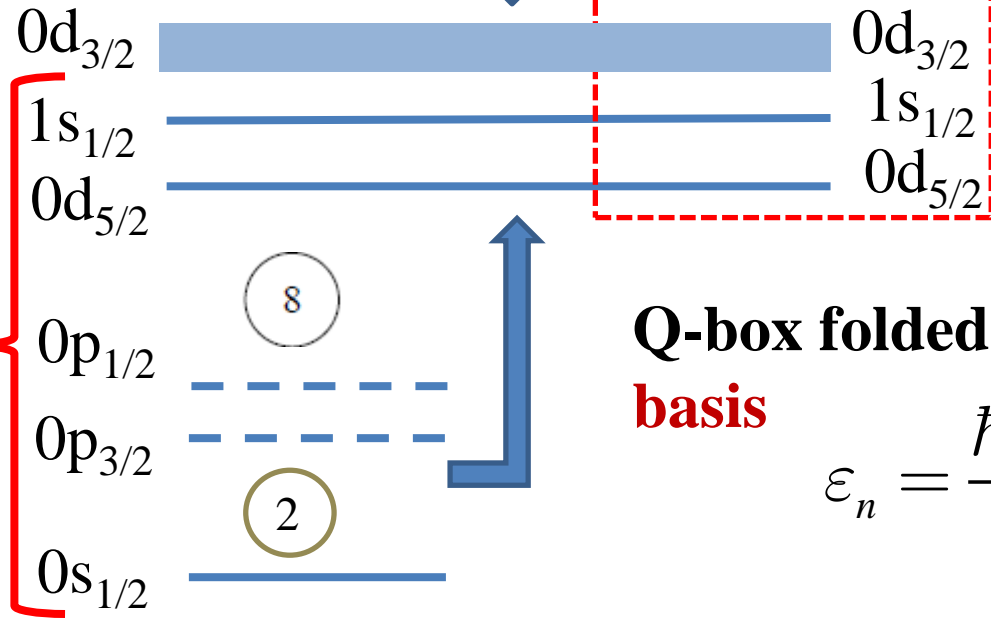
Continuum

For a given partial wave
(a given channel)

Berggren Completeness
Relation

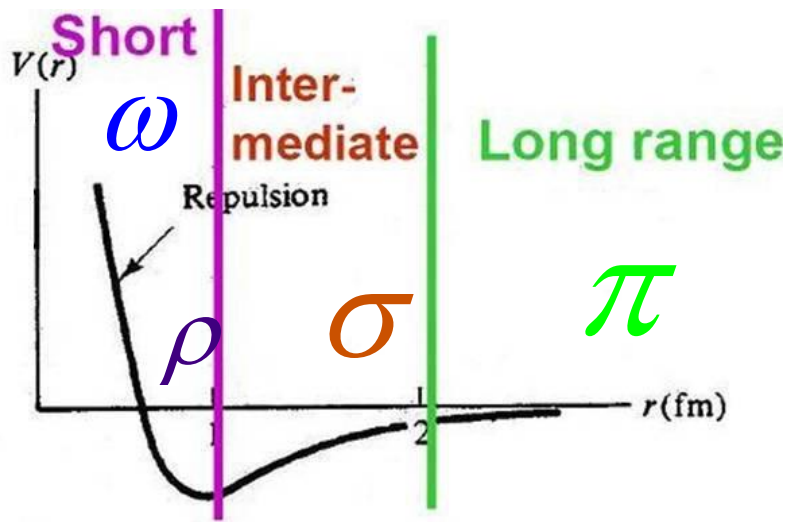
$$\sum_n |u_n\rangle \langle \tilde{u}_n| + \int_{L_+} |u_k\rangle \langle \tilde{u}_k| dk = 1$$

Bound



Q-box folded diagram in **complex-k**
basis

$$\epsilon_n = \frac{\hbar^2 k^2}{2m} = e_n - i \frac{\gamma_n}{2}$$



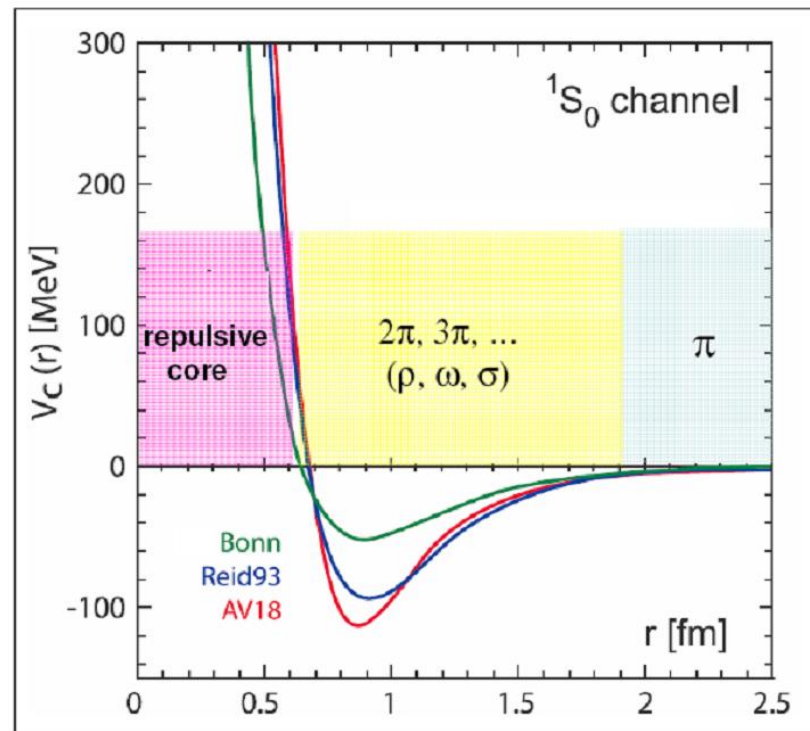
Meson-exchange potential

QCD-based Chiral effective field theory

(Chiral EFT)

Symmetries:

1. parity
2. spin
3. isospin

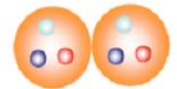


From T. Hatsuda (Oslo 2008)

One-pion exchange
by Yukawa (1935)



Multi-pions
by Taketani (1951)



Repulsive core
by Jastrow (1951)



Convergenes

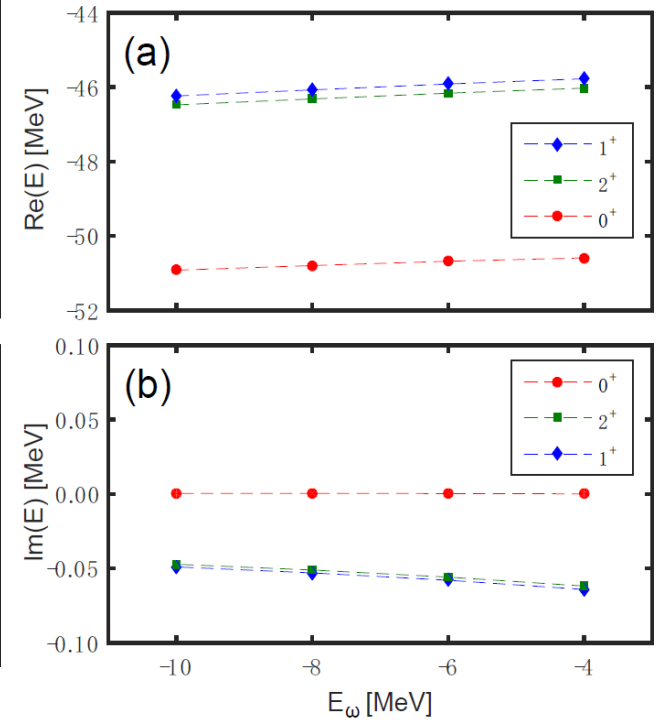
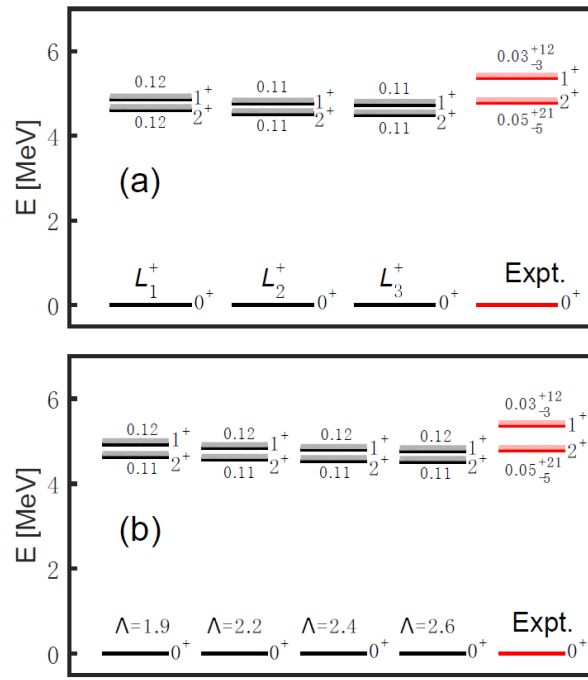
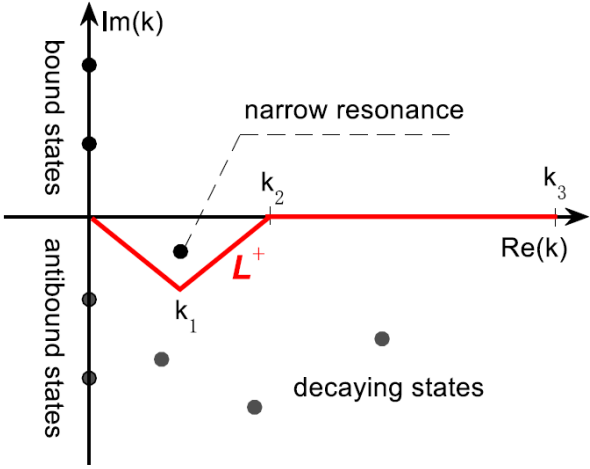
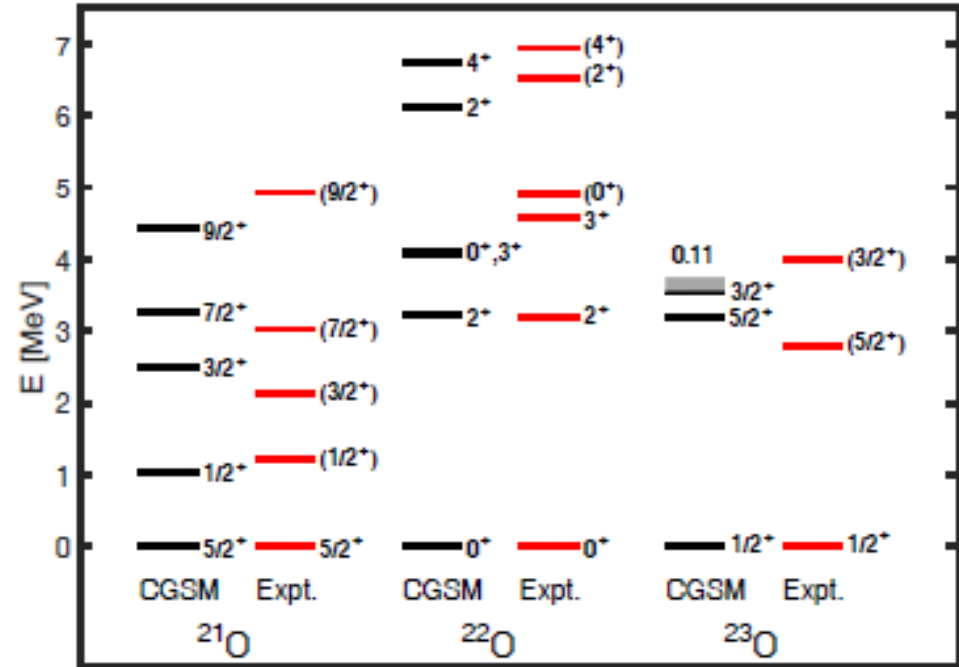
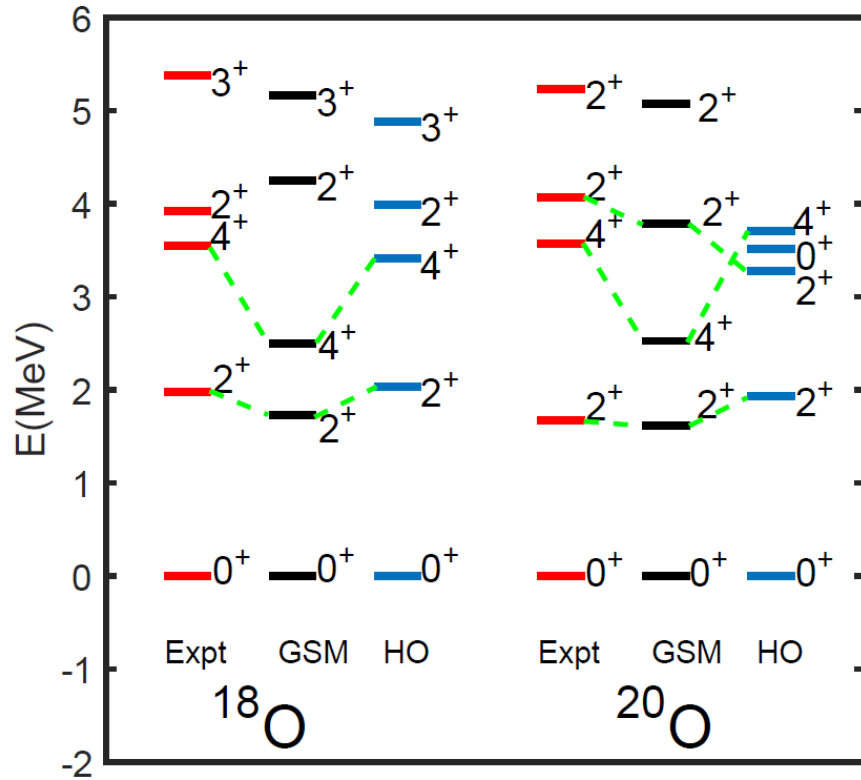


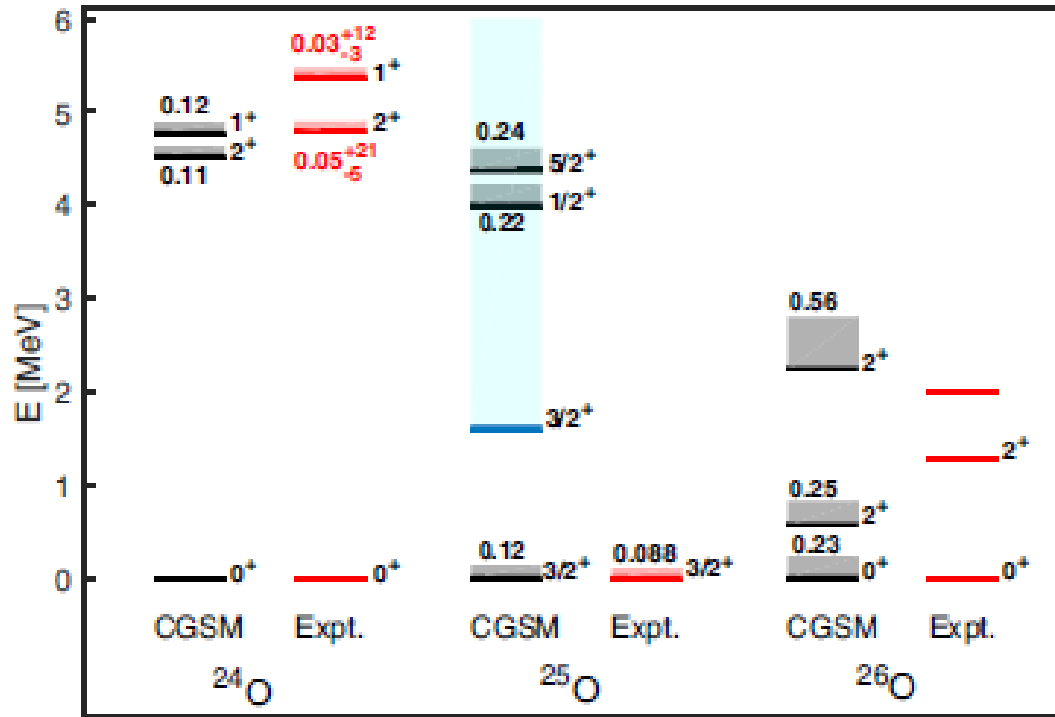
TABLE I. The convergences of the ^{24}O state energies $\tilde{E}_n = E_n - i\Gamma/2$ (in MeV) calculated with different discretization point numbers N_L on the $d_{3/2}$ continuum contour $L^+ = \{0.0 \rightarrow (0.48 - 0.20i) \rightarrow 0.62 \rightarrow 2.2\}$ (see Fig.1 for the definition of the contour L^+). $\Lambda = 2.6 \text{ fm}^{-1}$ is taken.

N_L	0^+	2^+	1^+
16	$-50.642 + 0.013i$	$-46.172 - 0.004i$	$-45.922 - 0.009i$
18	$-50.716 + 0.002i$	$-46.262 - 0.046i$	$-46.017 - 0.049i$
20	$-50.711 - 0.001i$	$-46.219 - 0.054i$	$-45.976 - 0.056i$
22	$-50.712 + 0.000i$	$-46.218 - 0.053i$	$-45.974 - 0.056i$

CD-Bonn CGSM, compared with conventional H.O. SM

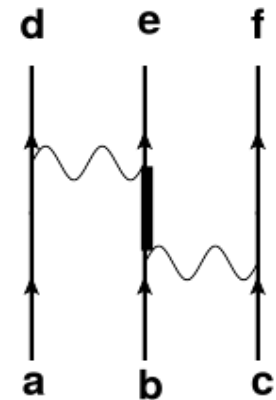


$(\Lambda=2.6 \text{ fm}^{-1})$



$(\Lambda=2.6 \text{ fm}^{-1})$

No 3-body force



Summary for CGSM calculations

1. Starting from the realistic nuclear force, CD-Bonn
2. $V_{\text{low-k}}$
3. Full Q-box folded-diagrams to build a realistic effective interaction for the defined non-degenerated model space
4. GSM with a doubly magic core
(resonance & continuum)
5. Well describe the spectra of bound, weakly-bound and unbound nuclei.

II. *ab-initio* calculations with MBPT

$$\hat{H}_{int} = \sum_{i<j}^A \frac{(\vec{p}_i - \vec{p}_j)^2}{2mA} + \sum_{i<j}^A V_{NN,ij} \quad ; \quad H_{int} = \sum_{i=1}^A \frac{p_i^2}{2m} + \sum_{i<j} V(|\vec{r}_i - \vec{r}_j|) - \frac{P^2}{2Am} \quad , \quad \vec{P} = \sum_{i=1}^A \vec{p}_i$$

- a) First we did HF calculations (in HO basis);
- b) The HF state is chosen as a reference state.
- c) In the HF basis, we make MBPT corrections up to 3rd order using *j-j* coupling:

$$H_0 = \sum_{l_1 l_2} h_{l_1 l_2}^{HF} a_{l_1}^\dagger a_{l_2}$$

$$\hat{H} = \hat{H}_0 + (\hat{H} - \hat{H}_0) = \hat{H}_0 + \hat{V}$$

The exact solutions of the A-nucleon system are,

$$\hat{H}\Psi_n = E_n\Psi_n, \quad n = 0, 1, 2, \dots$$

The zero-order part is,

$$\hat{H}_0\Phi_n = E_n^{(0)}\Phi_n, \quad n = 0, 1, 2, \dots$$

For the ground state:

$$\chi_0 = \Psi_0 - \Phi_0$$

$$\Delta E = E_0 - E_0^{(0)}$$

$$\Psi_0 = \sum_{m=0}^{\infty} [\hat{R}_0(E_0^{(0)})(\hat{V} - \Delta E)]^m \Phi_0$$

$$\Delta E = \sum_{m=0}^{\infty} \langle \Phi_0 | \hat{V} [\hat{R}_0(E_0^{(0)})(\hat{V} - \Delta E)]^m | \Phi_0 \rangle$$

where $\hat{R}_0 = \sum_{i \neq 0} \frac{|\Phi_i\rangle\langle\Phi_i|}{E_0^{(0)} - E_i^{(0)}}$ is called the resolvent of \hat{H}_0

Perturbation (MBPT)

Rayleigh-Schrodinger method

$$E_0 = E_0^{(0)} + E_0^{(1)} + E_0^{(2)} + E_0^{(3)} + \dots$$

$$\text{HF energy} = \langle \phi_0 | H | \phi_0 \rangle$$

$$E_0^{(1)} = \langle \phi_0 | \hat{V} | \phi_0 \rangle$$

$$E_0^{(2)} = \langle \phi_0 | \hat{V} \hat{R}_0 \hat{V} | \phi_0 \rangle$$

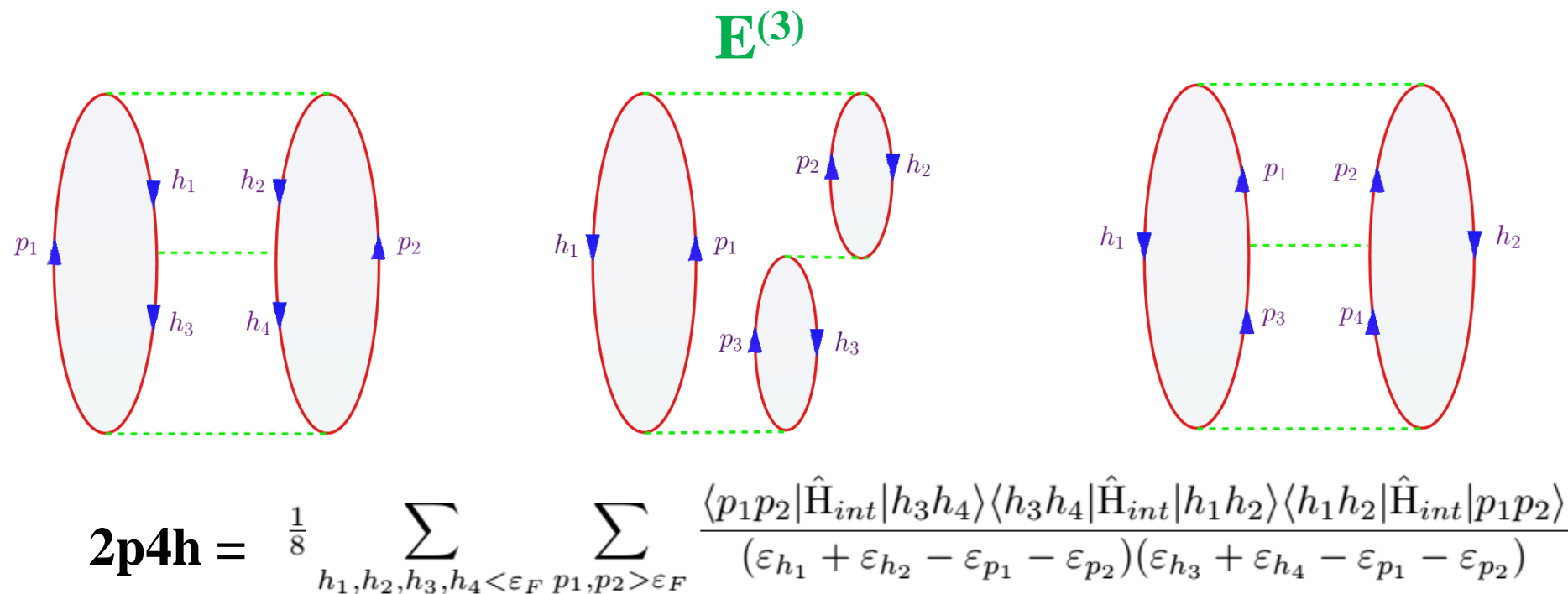
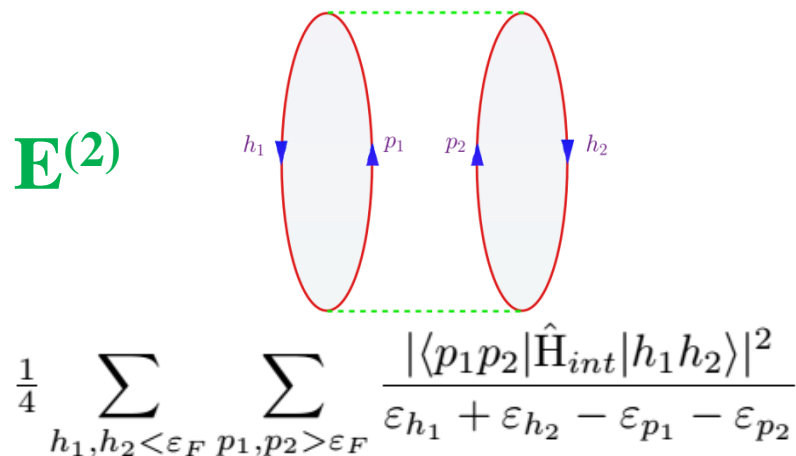
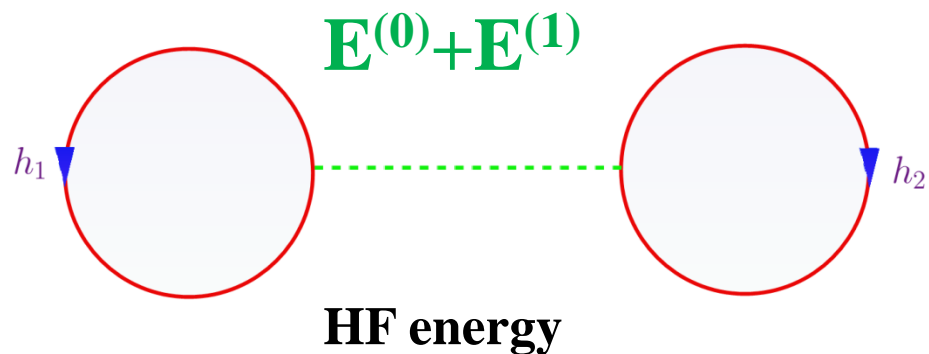
$$E_0^{(3)} = \langle \phi_0 | \hat{V} \hat{R}_0 (\hat{V} - \langle \phi_0 | \hat{V} | \phi_0 \rangle) \hat{R}_0 \hat{V} | \phi_0 \rangle$$

$$\psi_0 = \underbrace{\phi_0}_{\text{HF}} + \psi_0^{(1)} + \psi_0^{(2)} + \dots$$

$$\psi_0^{(1)} = \hat{R}_0 \hat{V} | \phi_0 \rangle$$

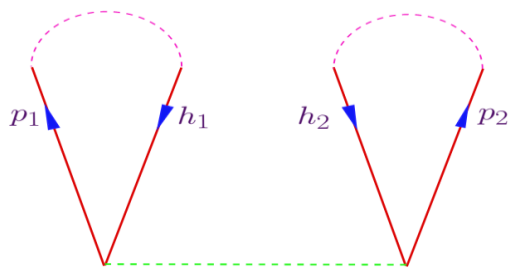
$$\psi_0^{(2)} = \hat{R}_0 (\hat{V} - E_0^{(1)}) \hat{R}_0 \hat{V} | \phi_0 \rangle$$

Anti-Symmetrized Goldstone (ASG) diagram expansion



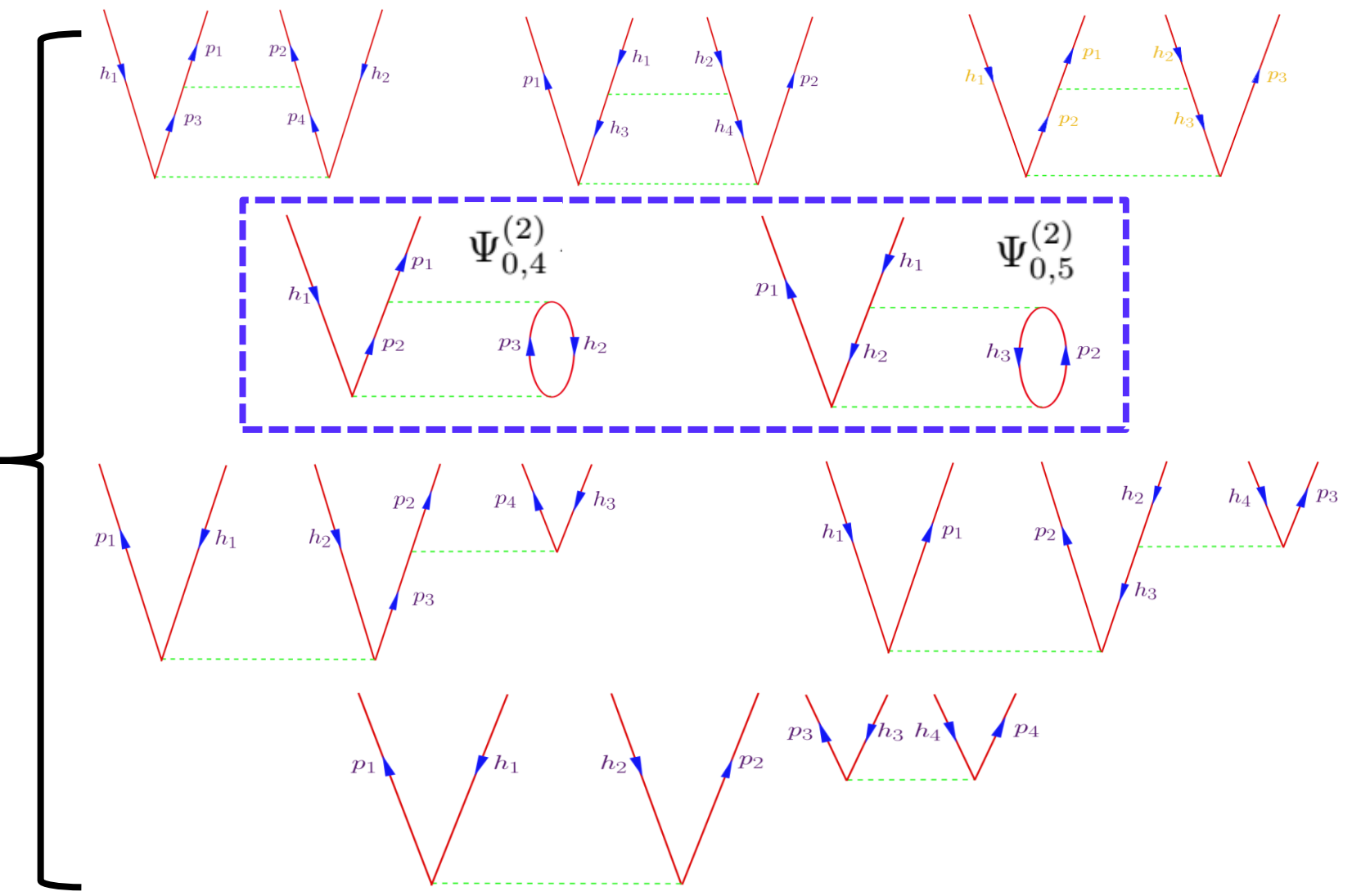
ASG diagrams for wave functions

$\psi^{(1)}$



$$\Psi'_0 = \Phi_0 + \Psi_0^{(1)} + \Psi_{0,4}^{(2)} + \Psi_{0,5}^{(2)}$$

$\psi^{(2)}$

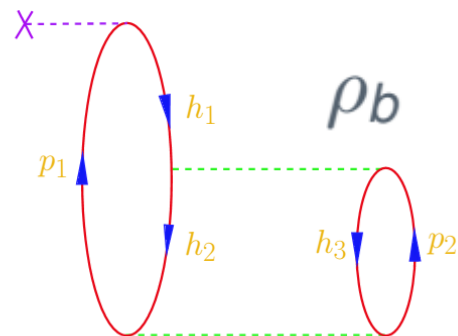
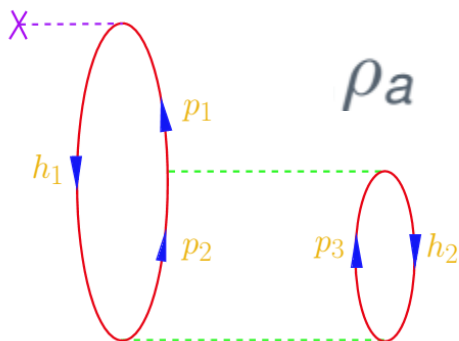


$$\rho(\vec{r}) = \underbrace{\langle \Phi_0 | \rho(\vec{r}) | \Phi_0 \rangle}_{\text{HF}} + \underbrace{\langle \Phi_0 | \rho(\vec{r}) | \Phi_0 \rangle \langle \Psi_0^{(1)} | \Psi_0^{(1)} \rangle}_{\text{2nd order}} + \underbrace{2\rho_a + 2\rho_b + \rho_{c1} + \rho_{c2} + \dots}_{\text{2nd order}}$$

HF

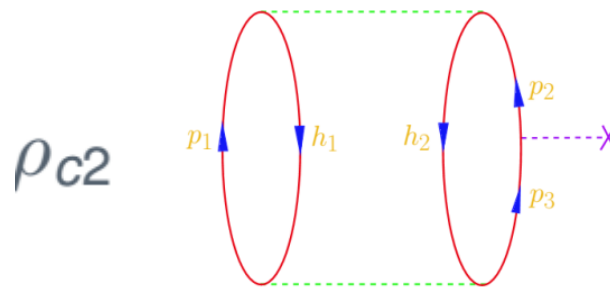
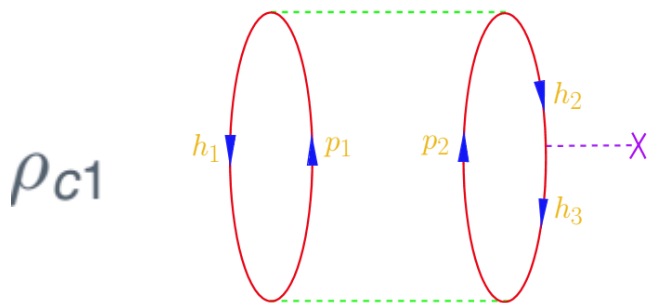
2nd order

2nd order



$$\frac{1}{2} \sum_{h_1, h_2 < \varepsilon_F} \sum_{p_1, p_2, p_3 > \varepsilon_F} \frac{\langle h_1 h_2 | \hat{H} | p_2 p_3 \rangle \langle p_2 p_3 | \hat{H} | p_1 h_2 \rangle \langle h_1 | \rho | p_1 \rangle}{(\varepsilon_{h_1} - \varepsilon_{p_1})(\varepsilon_{h_1} + \varepsilon_{h_2} - \varepsilon_{p_2} - \varepsilon_{p_3})}$$

$$-\frac{1}{2} \sum_{h_1, h_2, h_3 < \varepsilon_F} \sum_{p_1, p_2 > \varepsilon_F} \frac{\langle p_1 p_2 | \hat{H} | h_2 h_3 \rangle \langle h_2 h_3 | \hat{H} | h_1 p_2 \rangle \langle h_1 | \rho | p_1 \rangle}{(\varepsilon_{h_1} - \varepsilon_{p_1})(\varepsilon_{h_2} + \varepsilon_{h_3} - \varepsilon_{p_1} - \varepsilon_{p_2})}$$



$$-\frac{1}{2} \sum_{h_1, h_2, h_3 < \varepsilon_F} \sum_{p_1, p_2 > \varepsilon_F} \frac{\langle h_1 h_2 | \hat{H} | p_1 p_2 \rangle \langle p_1 p_2 | \hat{H} | h_1 h_3 \rangle \langle h_3 | \rho | h_2 \rangle}{(\varepsilon_{h_1} + \varepsilon_{h_2} - \varepsilon_{p_1} - \varepsilon_{p_2})(\varepsilon_{h_1} + \varepsilon_{h_3} - \varepsilon_{p_1} - \varepsilon_{p_2})}$$

$$\frac{1}{2} \sum_{h_1, h_2 < \varepsilon_F} \sum_{p_1, p_2, p_3 > \varepsilon_F} \frac{\langle p_1 p_3 | \hat{H} | h_1 h_2 \rangle \langle h_1 h_2 | \hat{H} | p_1 p_2 \rangle \langle p_2 | \rho | p_3 \rangle}{(\varepsilon_{h_1} + \varepsilon_{h_2} - \varepsilon_{p_1} - \varepsilon_{p_3})(\varepsilon_{h_1} + \varepsilon_{h_2} - \varepsilon_{p_1} - \varepsilon_{p_2})}$$

NCSM

S.K. Bogner *et al.*,

arXiv0708.3754v2 (2007)

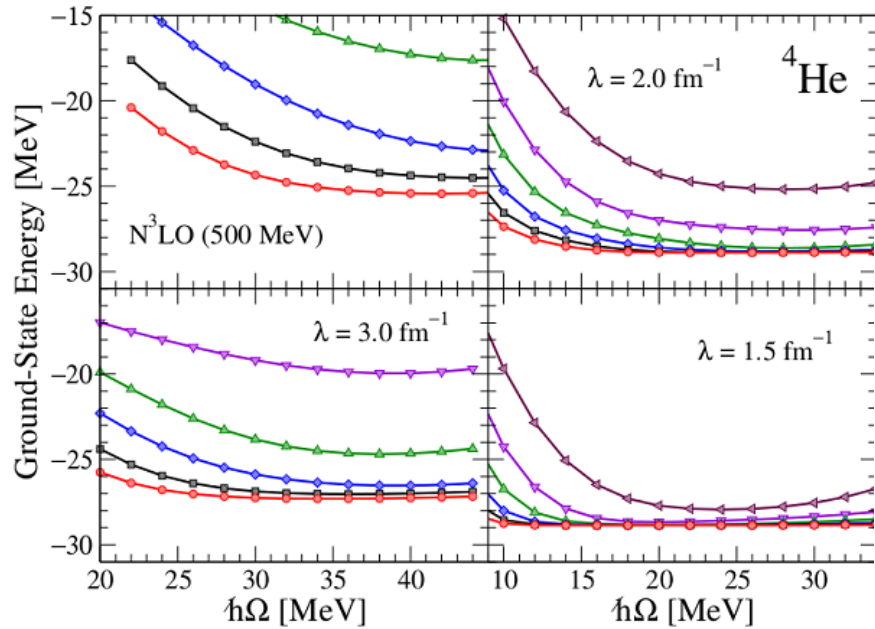
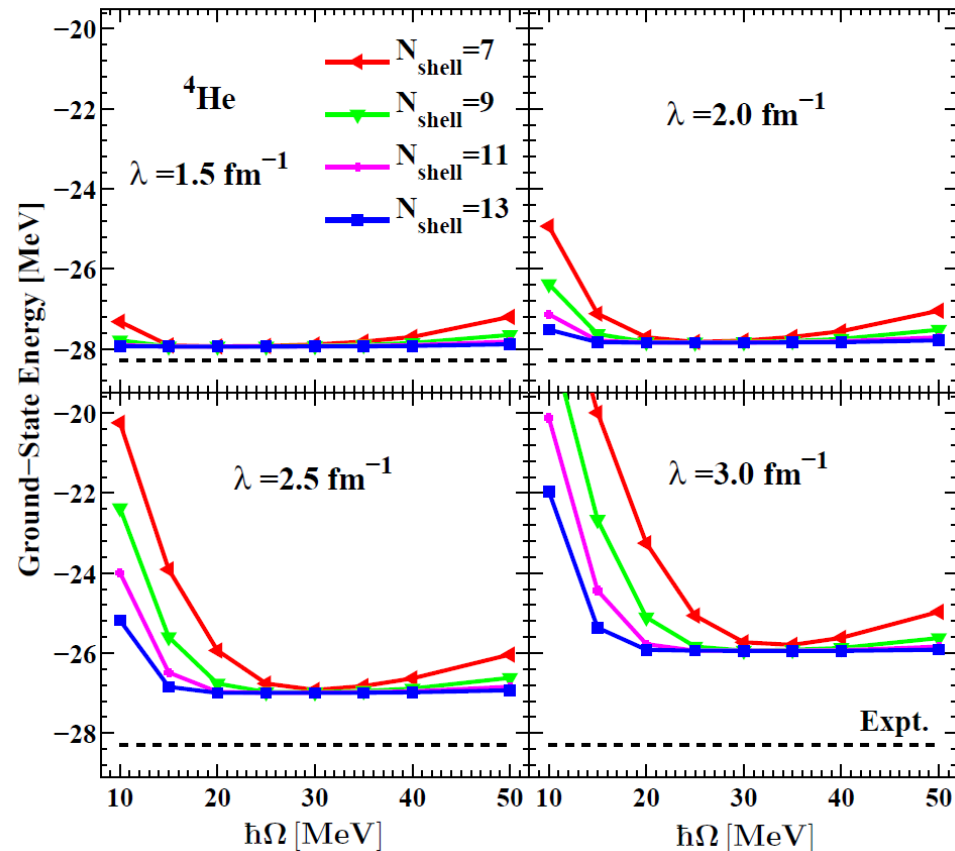


Fig. 3. Ground-state energy of ${}^4\text{He}$ as a function of $\hbar\Omega$ at four different value (∞ , 3, 2, 1.5 fm^{-1}). The initial potential is the 500 MeV N^3LO NN-only pot from Ref. [13]. The legend from Fig. 1 applies here.

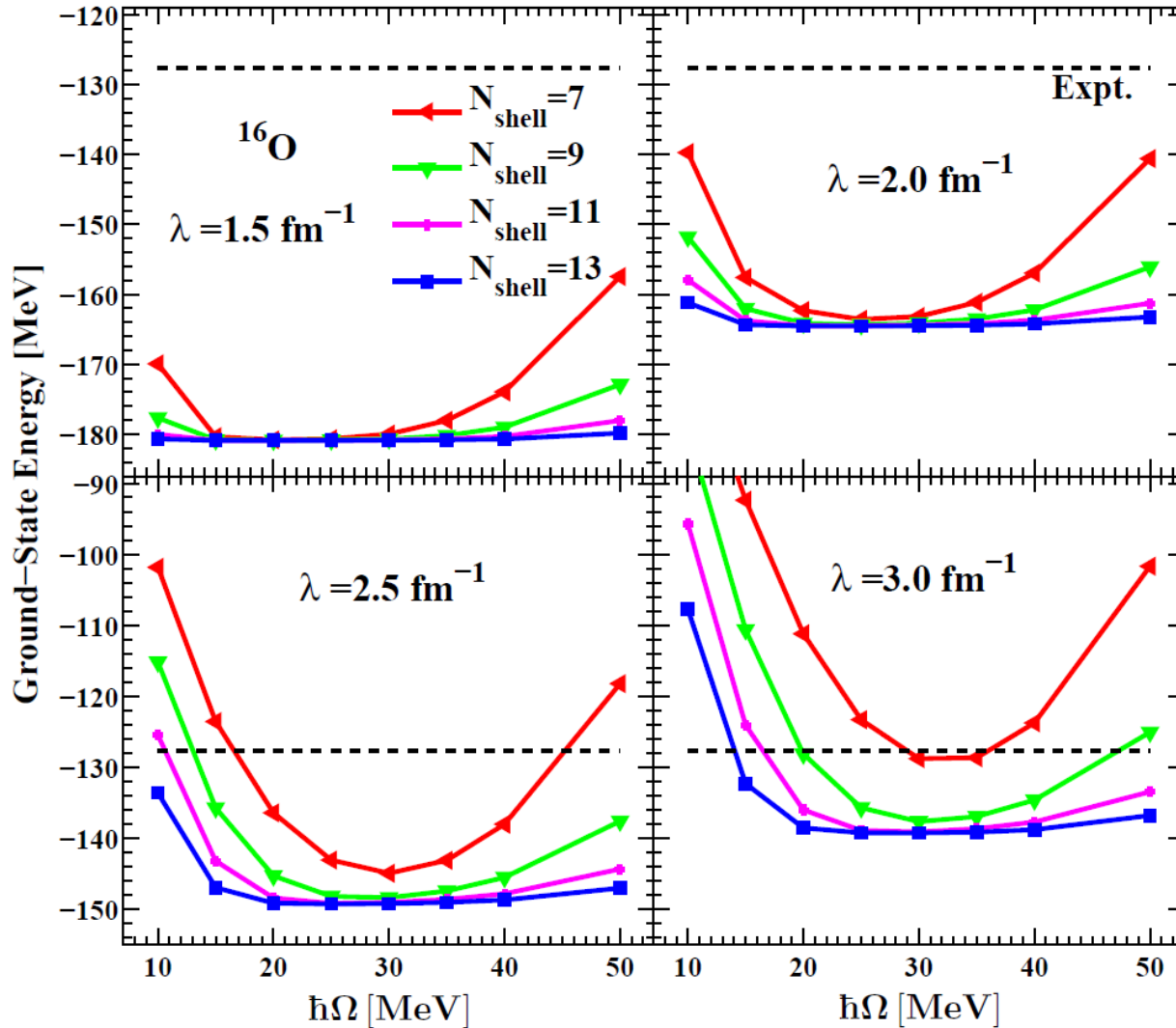
${}^4\text{He}$

Our MBPT calculations

$\text{N}^3\text{LO} + \text{SRG}$ without 3NF

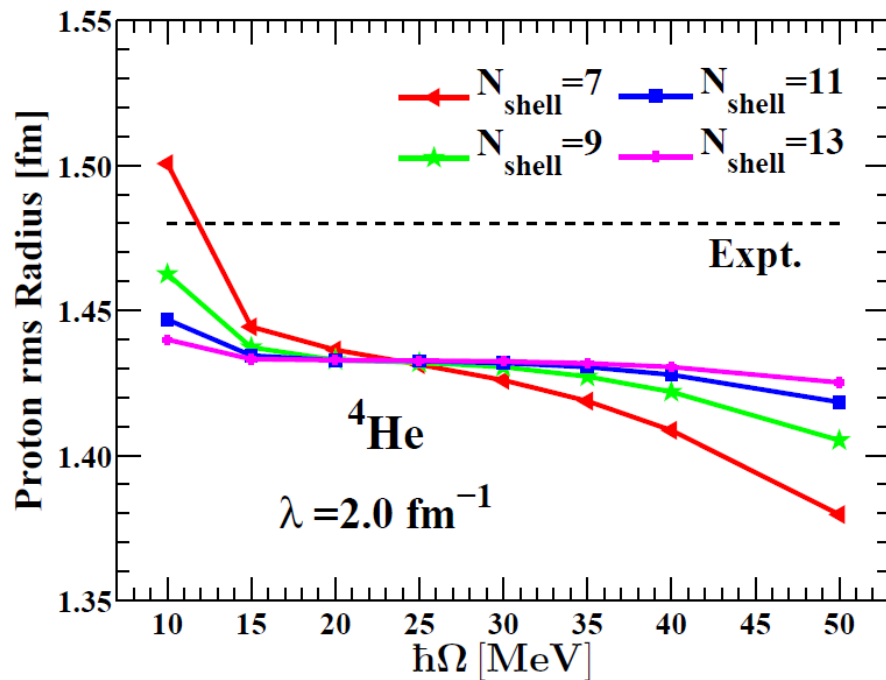
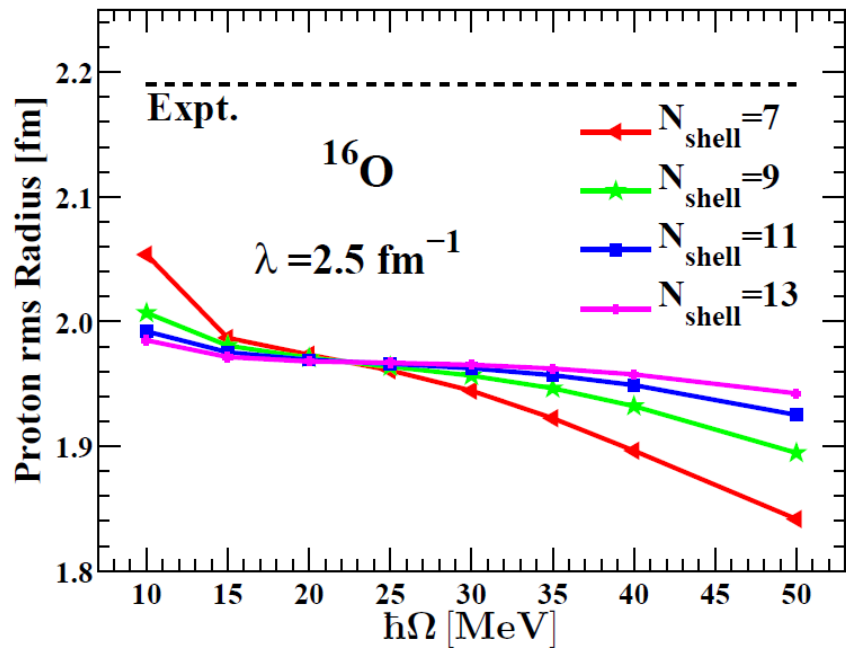


Our MBPT: $N^3\text{LO}+\text{SRG}$ without 3NF



^{16}O

Our MBPT calculations with N³LO+SRG: convergence in radius



R. Roth *et al.* (2006) PRC 73, 044312

AV18, UCOM, corrections to 3rd order in energy, 2nd order in radius

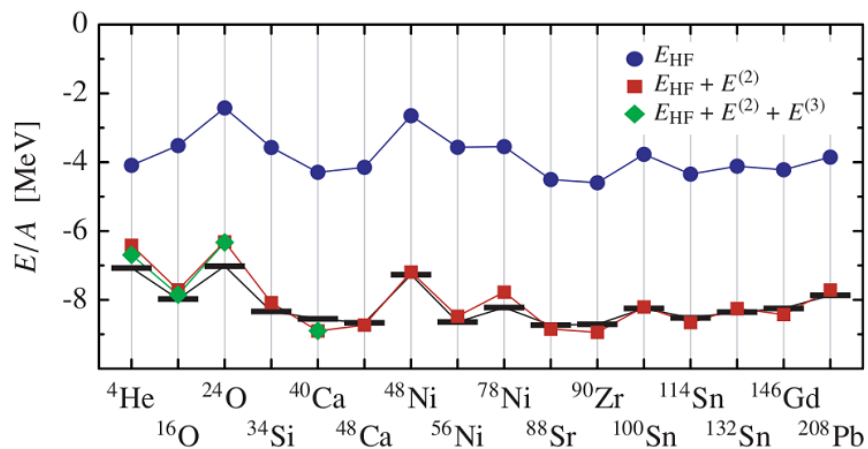


FIG. 5. (Color online) Ground-state energies for selected closed-shell nuclei in HF approximation and with added second- and third-order MBPT corrections. The correlated AV18 potential with $I_\vartheta = 0.09 \text{ fm}^3$ was used. The bars indicate the experimental binding energies [31].

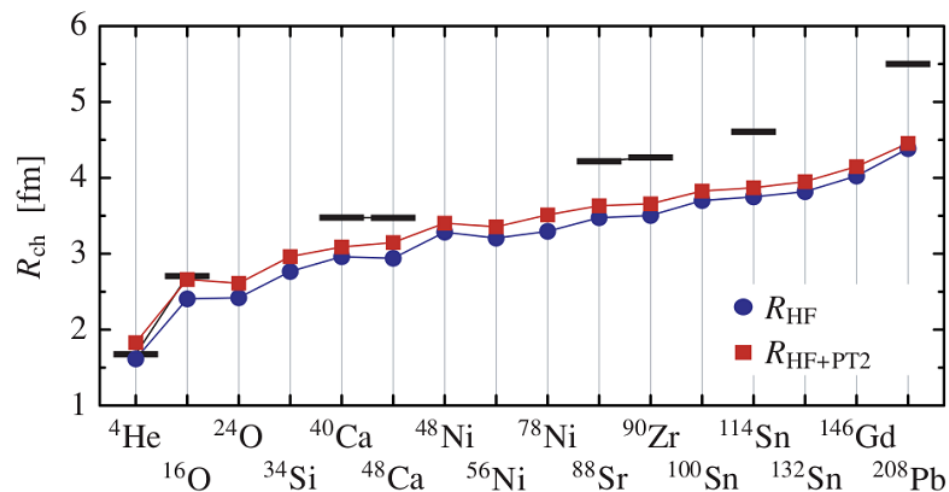


FIG. 8. (Color online) Charge radii for selected closed-shell nuclei in the HF approximation and with added second-order MBPT corrections. The correlated AV18 potential with $I_\vartheta = 0.09 \text{ fm}^3$ was used. The bars indicate experimental charge radii [32].

HF-MBPT calculations for ${}^4\text{He}$ with $\text{N}^3\text{LO-SRG}$, $\text{N}_{\text{shell}}=13$, $h\Omega=35$ MeV

		SRG flow parameter λ (fm $^{-1}$)			
		1.5	2.0	2.5	3.0
Expt. [60]		-28.296	-28.296	-28.296	-28.296
NCSM [61]		-28.20	-28.41	-27.43	-26.80
Binding energy	SHF	-25.754	-21.864	-15.854	-10.278
	PT2	-1.788	-5.088	-9.652	-13.783
	PT3	-0.391	-0.899	-1.523	-1.953
	SHF+PT2+PT3	-27.933	-27.850	-27.029	-26.013

$r_p(\text{NCSM})=1.418$ fm with $\text{N}_{\text{max}}=10$

		SRG flow parameter λ (fm $^{-1}$)			
		1.5	2.0	2.5	3.0
Expt.		1.477	1.477	1.477	1.477
Point-proton rms radius	SHF	1.677	1.652	1.714	1.816
	PT2	0.007	0.001	-0.021	-0.065
	$\Delta r_{\text{c.m.}}$	-0.226	-0.222	-0.227	-0.235
	SHF+PT2+ $\Delta r_{\text{c.m.}}$	1.458	1.431	1.466	1.516

HF-MBPT calculations for ^{16}O with $\text{N}^3\text{LO-SRG}$, $N_{\text{shell}}=13$, $\hbar\Omega=35$ MeV

		SRG flow parameter λ (fm^{-1})			
		1.5	2.0	2.5	3.0
Binding energy	Expt. [60]	-127.619	-127.619	-127.619	-127.619
	SHF	-169.968	-133.169	-85.173	-44.102
	PT2	-10.132	-29.497	-59.617	-88.326
	PT3	-0.794	-1.931	-4.630	-7.339
	SHF+PT2+PT3	-180.893	-164.597	-149.419	-139.767

3NF important!

		SRG flow parameter λ (fm^{-1})			
		1.5	2.0	2.5	3.0
Point-proton rms radius	Expt.	2.581	2.581	2.581	2.581
	SHF	2.098	2.096	2.201	2.345
	PT2	0.011	0.011	-0.006	-0.042
	$\Delta r_{\text{c.m.}}$	-0.067	-0.067	-0.070	-0.073
	SHF+PT2+ $\Delta r_{\text{c.m.}}$	2.042	2.040	2.125	2.230

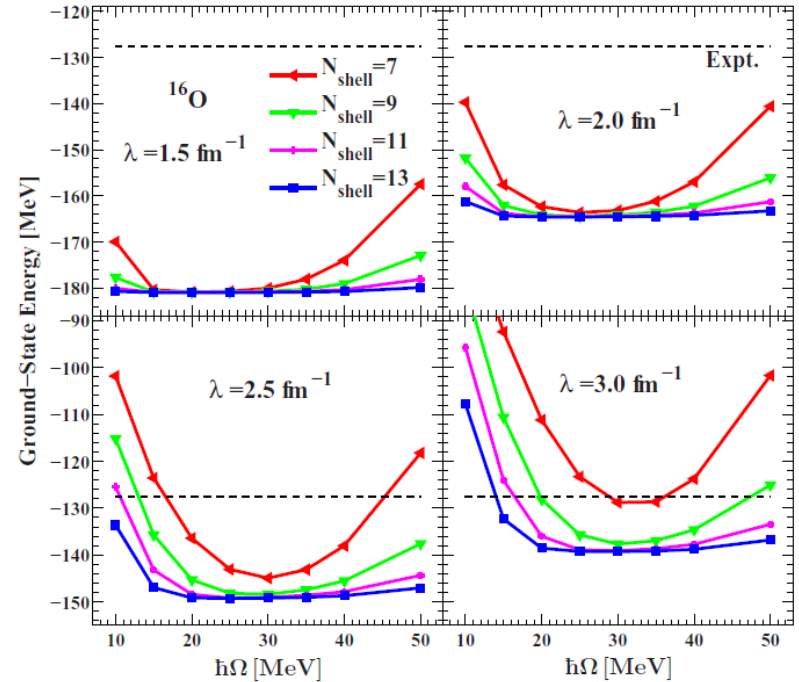
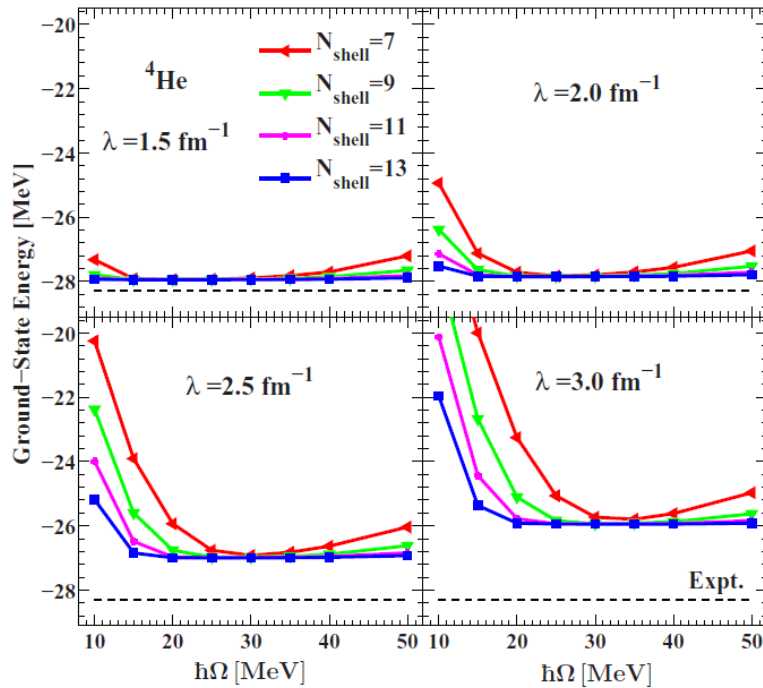
Ab initio nuclear many-body perturbation calculations in the Hartree-Fock basis

B. S. Hu (胡柏山),¹ F. R. Xu (许甫荣),^{1,*} Z. H. Sun (孙中浩),¹ J. P. Vary,² and T. Li (李通)¹

¹State Key Laboratory of Nuclear Physics and Technology, School of Physics, Peking University, Beijing 100871, China

²Department of Physics and Astronomy, Iowa State University, Ames, Iowa 50011, USA

(Received 25 April 2016; published 6 July 2016)



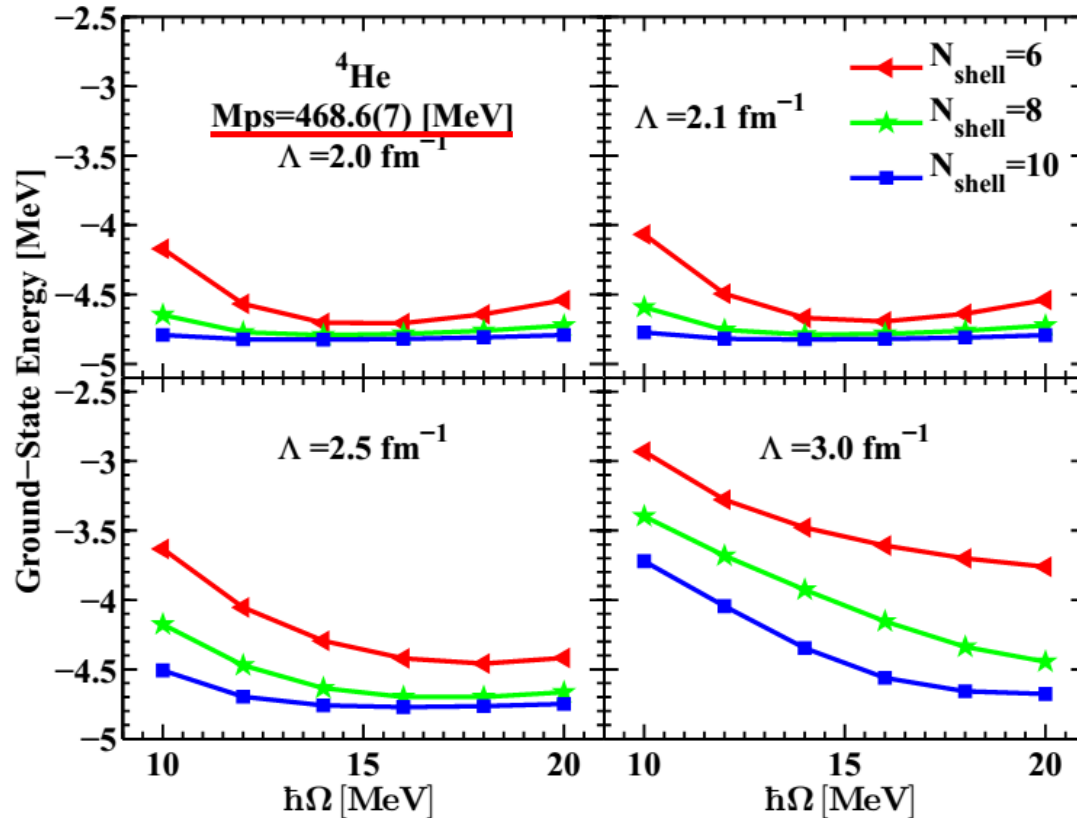
Chiral potential $N^3\text{LO}$ MBPT calculations

LQCD \rightarrow MBPT calculations

LQCD was provided by Aoki and Inoue

We renormalize it using $V_{\text{low-k}}$

Preliminary



$E^{\text{expt}} = -28.3 \text{ MeV}$

FIG. 6. Ground-state energy of ${}^4\text{He}$ in MBPT calculation as a function of oscillator parameter $\hbar\Omega$ for different V_{lowk} interactions with $\Lambda = 2.0, 2.1, 2.5, 3.0 \text{ fm}^{-1}$. The initial interaction is the lattice QCD simulations [1–4].

Preliminary

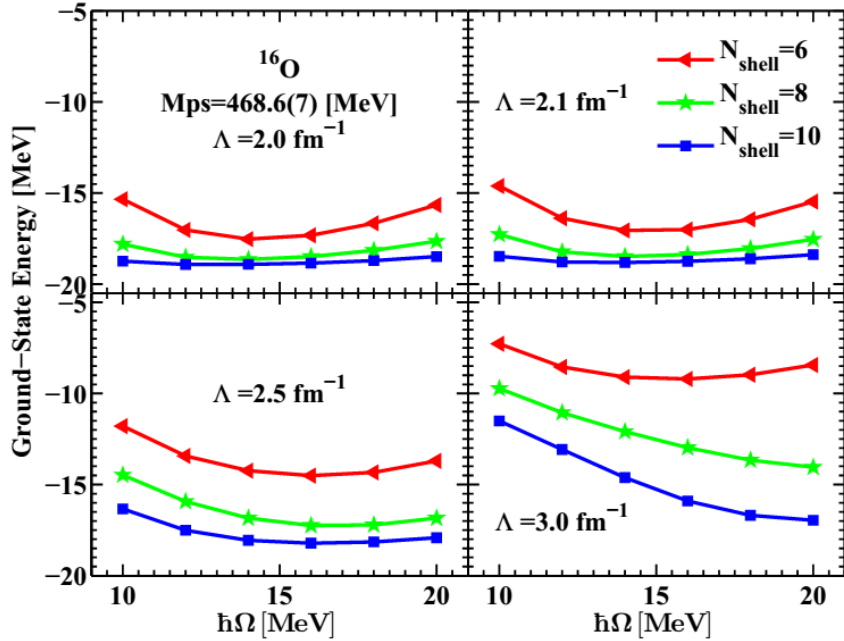


FIG. 7. Ground-state energy of ^{16}O in MBPT calculation as a function of oscillator parameter $\hbar\Omega$ for different V_{lowk} interactions with $\Lambda = 2.0, 2.1, 2.5, 3.0 \text{ fm}^{-1}$. The initial interaction is the lattice QCD simulations [1-4].

$$E^{\text{expt}} = -127.6 \text{ MeV}$$

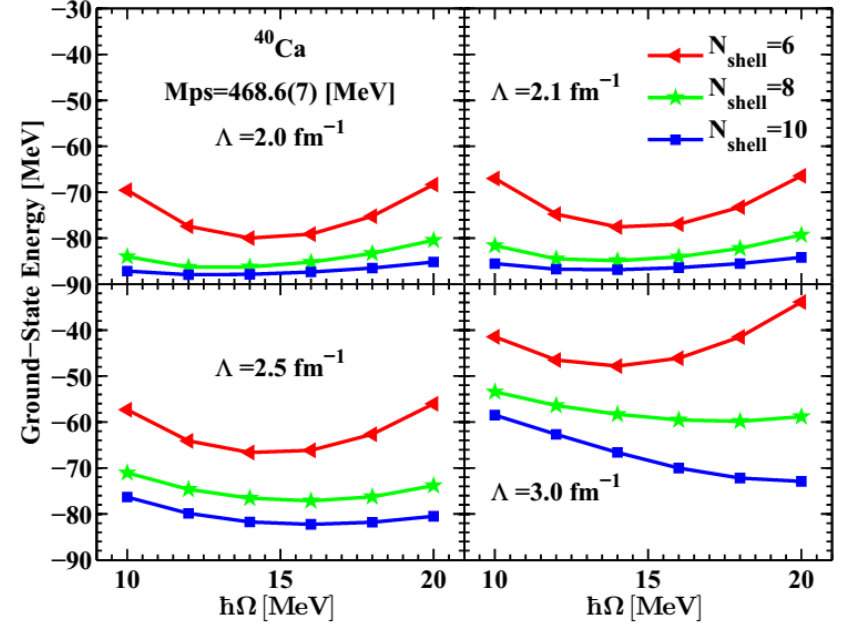


FIG. 8. Ground-state energy of ^{40}Ca in MBPT calculation as a function of oscillator parameter $\hbar\Omega$ for different V_{lowk} interactions with $\Lambda = 2.0, 2.1, 2.5, 3.0 \text{ fm}^{-1}$. The initial interaction is the lattice QCD simulations [1-4].

$$E^{\text{expt}} = -342.0 \text{ MeV}$$

III. Summary

Starting with realistic nuclear forces

- I. CGSM with CD Bonn + $V_{\text{low } k}$ +folded-diagram for weakly-bound and unbound nuclei (resonance & continuum), **Oxygen isotopes**
- II. MBPT with $N^3\text{LO}$ (LQCD) + SRG for **close-shell nuclei**

Advantages of *ab-initio* calculations:

- i) To understand the nature of nuclear forces;
- ii) To understand many-body correlations;

.....

Collaborators:

Peking University:

Zhonghao Sun, Baishan Hu, Qiang Wu, Sijie Dai , T. Li

Zhenhao Zhao, Junchen Pei

Iowa State University:

James Vary

Thanks to:

Sinya Aoki and Takashi Inoue;

Bruce Barrett, Luigi Coraggio, Rup Machleidt, Thomas Papenbrock

Thank you for your attention

NTSE–2016, Khabarovsk, 19-23 September, 2016, Khabarovsk, Russian